A novel punch design approach with progressive clearance variation for the punching–broaching process

S F Lajarin, R C B Neto, A M Eto, and **P V P Marcondes***
Department of Mechanical Engineering, Federal University of Paraná, Curitiba, Brazil

The manuscript was received on 20 May 2011 and was accepted after revision for publication on 1 September 2011.

DOI: 10.1177/0954405411424239

Abstract: Thick sheet punching is a process used in the automobile industry, especially in the heavy vehicles segment. Aimed at generating holes of good cylindricity and surface quality, the definition of the process parameter values and the tool design are critical to the process. For this purpose, the finite element method is useful to decrease the trial-and-error procedures and also the tool development costs. The main aim of the present study was to analyse the influence of the punch design on the final quality of punched/broached holes produced on thick steel sheets (8 mm, NBR 6656). Several geometries of punch with combined broaching teeth as well as punches with traditional geometries have been analysed. The results of the simulations led to a detailed understanding of the influence of punch geometry during the punching–broaching process. In addition, a novel punch design approach was proposed which allowed the production of holes of good cylindricity due to the progressive variation of the clearance between the punch and the die during the punch penetration progress.

Keywords: punching and broaching, progressive clearance variation, tool design

1 INTRODUCTION

Thick sheet punching is a process used in the truck, car, and tractor production industries and the petroleum segment. This process consists of cutting the metallic sheet through the application of shearing tensions by a punch against a rigid die. The shearing tensions originate from superficial cracks whose onset takes place at the regions in contact with the punch–die interface. The punch penetration progression propagates the crack, resulting in the complete rupture of the material.

The choice of suitable parameters for the tool and for the process is crucial to the quality of the punched hole, albeit the identification of these parameters is, in general, the result of a series of experiments which are costly and time demanding. This fact was stated by Al-Momani and Rawabdeh [**1**], who concluded that use of the finite element method (FEM), coupled with design of experiments, provides a good contribution towards optimization of the sheet metal punching and blanking process.

In past years, simulations of the shearing process of sheet metals have been carried out emphasizing use of the FEM to help the trial-and-error procedures and also bringing about a better understanding of the effects of process parameters. Hatanaka *et al.* [**2**] carried out a series of blanking experiments where the deformation aspect of the material in the shearing region was observed in detail. From their studies it was concluded that the penetration depth at the crack initiation depends on the clearance between the punch and the die. In cases when the clearance is small, the cracks generated from the punch and die edges propagate along a straight line connecting the tips of both cracks, i.e. the punch penetration depth at the crack onset becomes larger as the clearance increases. FEM simulations have confirmed such results. Husson *et al.* [**3**] also conducted studies with FEM simulations of a blanking process and found that, at high clearance, high tool

**Corresponding author: Universidade Federal do Paraná, DEMEC, Av. Cel. Francisco H. dos Santos 210, CEP 81531-990, Curitiba, Paraná, Brazil, CP 19011.*
email: marcondes@ufpr.br

wear (due to the high friction condition) affects the quality of predicted sheared edges. Soares *et al.* [**4**] studied the influence of the clearance between punch and die during punching, via FEM. They reported that clearances between 2 and 10 per cent were suitable for ductile steels because these materials need a smaller punch force and do not produce large burrs during the punching process. Hambli [**5**] reported a comparative study in prediction of burr height formation in the blanking process and showed that the results obtained by simulation and by experimentation were similar. He reported that clearances up to 10 per cent are suitable to minimize cutting forces; nevertheless, clearances up to 5 per cent are desirable because the fracture angle and depth developed at the cutting region are minimized. When clearance is set at 10 per cent, the process is slightly more robust to tool wear as far as the blanking force response is concerned and it is considerably more robust – almost insensitive – to tool wear and sheet thickness as far as the fracture depth response is concerned. Whether clearance should be set at 5 per cent or 10 per cent ultimately depends on the priorities of the practitioners [**6**]. Marouani *et al.* [**7**] studied the punch velocity (strain rate) and clearance effect on the shearing process by experimental and numerical investigations. Conventional mechanical machines such as crank presses operate at speeds ranging from 0.06 to 1.5 m/s. The authors concluded from their study that both the maximum punch force and the shape of the cut edge are affected by the punch velocity. In addition, they reported that numerical simulation can be a useful tool not only to improve the process, but also to describe the material elastic–plastic behaviour during punching and to assess tool changes. Komori [**8**] studied the ductile damage in metallic sheets experimentally and by FEM, developing a computer finite element program which showed the crack growth behaviour after the ductile fracture. Farzin *et al.* [**9**] evaluated the influence of various damage criteria in the simulation of the blanking process and achieved a good match with experimental data.

Singh *et al.* [**10**] performed a design study of the geometry of a punching–blanking tool using FEM simulations, aimed at reducing the stress at the tool during the punching/blanking process. A comparison of different punch geometries was carried out and the effects of tool geometry on the punching–blanking force and deformation of the punch were analysed. However, it can be noted that there are few studies in the literature on punching or blanking of thick sheets using numerical simulation – despite the process being used industrially. Observing this research gap, Mello and Marcondes [**11**] reported a new perforating process via a punching–broaching combined tool, i.e. a tool with a punch tip and broaching teeth at its body. In order to study the feasibility of this new combined tool for punching and broaching, Marcondes *et al.* [**12**] studied experimentally the geometry of the tool broaching area, the use of the punch tip for cutting, and the lubrication effects as control variables.

In order to advance the subject a little further and as a contribution to the research gap still present in the state-of-the-art, the current work aimed to analyse, via numerical simulation, the influence of the punch geometry on the quality of punched holes for thick steel sheets. In order to do so, the influence of the geometric configuration of the punches proposed by Marcondes *et al.* [**12**] on the quality of holes produced by punching of thick sheet was first analysed. Then, a numerical study was conducted with four different shapes to complement the analysis of the influence of geometry in the process of punching. Finally, based on the results, a novel punch geometry that combines the major advantages of the previously studied punches was proposed.

2 EXPERIMENTAL PROCEDURE

The original experimental setup and quantitative evaluation using analysis of variance of the hole surface quality and dimensional precision (i.e. roughness, fracture angle, tool temperature, and tool degradation) for the new perforating process via the punching–broaching combined tool were reported elsewhere [**12**]. The experimental data were used to validate the numerical simulations of the present work.

To assess the effective influence of the broaching operation of the tool developed by Marcondes *et al.* [**12**], three punches with different geometries of the tool broaching area were evaluated in the present work via FEM, using plane shear and the same friction conditions. The tool geometries I, II, and III and their dimensions are shown in Fig. 1. The type I punch has progressive teeth only in the cutting direction, whereas the type II punch has progressive teeth in both cutting and withdrawal directions, and the type III punch has progressive teeth in the cutting direction in two segments (2×). Geometrically, the tools have 100 mm length and initial diameter of 8.8 mm with the goal to punch holes with 10 mm final diameter. The die diameter is 10.02 mm, i.e. the clearance between the initial diameter of the punch and the die is about 7.6 per cent of the sheet thickness per side.

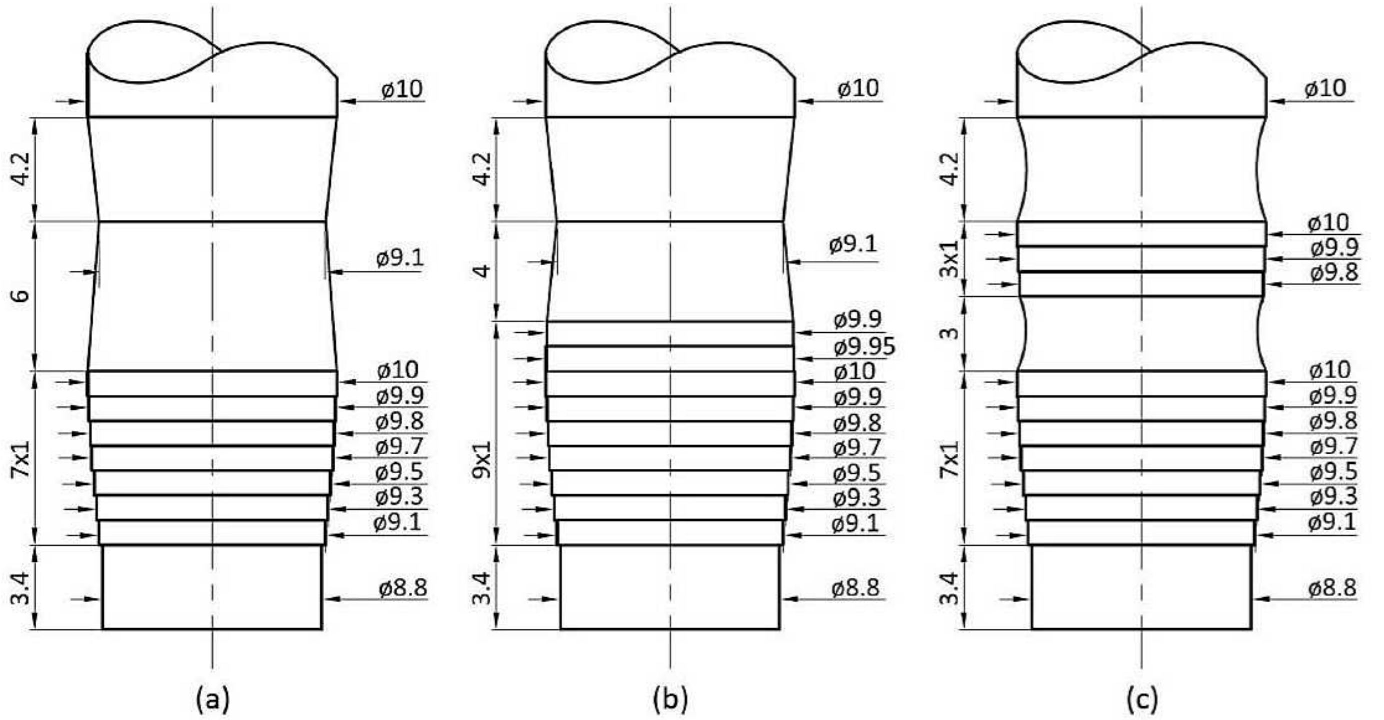

Fig. 1 Punch tool geometries (all dimensions in mm): (a) type I; (b) type II; (c) type III

The simulation of the combined punching and broaching process was performed through the commercial FEM code ABAQUS/Explicit using an axisymmetric model. The sheet was meshed with quadrilateral elements with four nodes and reduced integration (type CAX4R) and triangular elements with three nodes (type CAX3) [**13**]. Söderberg [**14**] reported that 128 mesh elements in the thickness can provide good results. In the present work, in the areas under high stresses (shear region), 128 mesh elements were applied in the sheet thickness and a coarse mesh was used for areas not under high stress levels. The punch, die, and blank holder were considered as analytic rigid surfaces. The contact between the sheet and the tools was described by the Coulomb friction model with a friction coefficient of 0.1 in all simulations. The load at the blank holder was 10 000 N and the punch velocity was 1 m/s.

The sheet material used was 8 mm thick, high-resistance NBR 6656 steel. Its mechanical properties are shown in Table 1.

The material was modelled as von Mises isotropic hardening – assuming the material properties to be similar in all directions. The damage initiation criteria were chosen so as to predict the damage initiation due to nucleation, growth, and coalescence of voids in ductile materials. The model assumes that the equivalent plastic strain at the beginning of failure, $\dot{\bar{\varepsilon}}_{\mathrm{D}}^{\mathrm{pl}}$, is a function of the triaxial stress and the strain rate, $\dot{\bar{\varepsilon}}_{\mathrm{D}}^{\mathrm{pl}}(\eta, \dot{\bar{\varepsilon}}^{\mathrm{pl}})$. In this case, $\eta = -p/q$ is the triaxiality stress, where p is the pressure stress, q is the von Mises equivalent stress, and $\dot{\bar{\varepsilon}}^{\mathrm{pl}}$ is the equivalent plastic strain rate. The pressure stress p and the von Mises equivalent stress q are represented by equations (1) and (2), respectively

$$p = \frac{1}{3}(\sigma_1 + \sigma_2 + \sigma_3) \tag{1}$$

$$q = \frac{1}{\sqrt{2}}\left[(\sigma_1 - \sigma_2)^2 + (\sigma_2 - \sigma_3)^2 + (\sigma_3 - \sigma_2)^2\right]^{1/2} \tag{2}$$

The criterion for damage initiation proposed by Wu [**15**] is achieved when the condition shown in equation (3) is satisfied, where $\bar{\omega}_{\mathrm{D}}$ is a state variable that increases monotonically with plastic strain. At each increment, the incremental growth in $\bar{\omega}_{\mathrm{D}}$ is computed with equation (4)

Table 1 Mechanical properties of NBR 6656 steel

Yield strength (MPa)	Tensile strength (MPa)	Elongation (%)	K (MPa)	n	Density (kg/mm^3)	Poisson's ratio	Elastic modulus (MPa)
439	521	29	1012	0.20	7.8×10^9	0.3	210 000

$$\bar{\omega}_D = \int \frac{d\bar{\varepsilon}^{pl}}{\bar{\varepsilon}_D^{pl}(\eta, \dot{\bar{\varepsilon}}^{pl})} = 1 \quad (3)$$

$$\Delta\bar{\omega}_D = \frac{\Delta\bar{\varepsilon}^{pl}}{\bar{\varepsilon}_D^{pl}(\eta, \dot{\bar{\varepsilon}}^{pl})} \geqslant 0 \quad (4)$$

In the simulations, it was assumed that stiffness degradation is associated with each ductile damage mechanism and can be modelled by applying a scalar damage variable, D. At any given loading cycle during the analysis the stress tensor in the material is given by the scalar damage (equation (5))

$$\sigma = (1 - D)\bar{\sigma} \quad (5)$$

where $\bar{\sigma}$ is the effective (or undamaged) stress tensor that would exist in the material in the absence of damage computed in the current increment. The material loses its load-carrying capacity completely when $D = 1$.

The data considered to define the ductile damage mechanism can be obtained as follows. For the uniaxial stress, $\sigma_2 \neq 0$, $\sigma_1 = \sigma_3 = 0$, the triaxial stress factor value is obtained by replacing the values $\sigma_2 \neq 0$, $\sigma_1 = \sigma_3 = 0$ in equations (1) and (2) and $\eta = 0.272$ is obtained. For the biaxial stress, it is assumed that $\sigma_1 = \sigma_2$ and $\sigma_3 = 0$ and $\eta = 0.667$ is calculated. For shearing, $\sigma_1 = -\sigma_2$ and $\sigma_3 = 0$ and $\eta = 0$ is obtained. Furthermore, the damage evolution criterion was determined, i.e. the parameter that defines how the material degrades after the damage initiation criteria are found.

3 RESULTS

The broaching teeth of the type I punch machined the hole wall leaving a rough conic region (1 mm) at the bottom end of the hole and a small burr (see Fig. 2(a)). Owing to the cutting geometry in the opposite direction (type II) and in two sections (type III), the other punches pulled the burr material inside the hole during the punch withdrawal. As can be observed (Figs 2(b) and (c)), the hole wall is divided into two regions: the superior machined during the downwards movement of the punch and the inferior machined during the punch withdrawal.

Figure 2 shows that the variation in the arrangement and amount of broaching teeth on the type II and III punches did not cause any differences in wall quality and only a small difference in roughness was observed for the holes obtained with the type I punch. However, the geometric differences between the punches produced variations in the force required during the stroke. The hole surface quality obtained experimentally and the numerical data showed good agreement.

Figure 3 illustrates the force–stroke diagram for the three types of punch. For all cases studied, the force peak occurred just before the start of the crack on the die edge. In all cases, the peak force was about 140 kN. After the maximum force peak, the cracks spread and met, producing the blow-out effect. In all cases, the failure was around 2.6 mm stroke (one-third of the sheet thickness). A clearance between the punch and die above 7 per cent led to a bigger fracture angle. After the blow-out effect, the broaching teeth began to machine the hole wall and improve its roundness. The action of the broaching teeth also showed variation in the required force. The type II punch data (Fig. 3(b)) illustrated a second force peak that occurred when the last tooth machined the hole wall. It is worthy of note that punch type II has two broaching teeth in order to machine the wall during the punch withdrawal. The force curve showed only a slight variation at the beginning of the punch withdrawal, possibly due to the fact that the teeth designed to machine at the withdrawal are not acting as expected, but pulling burr material into the hole. According to the simulation results holes with good finishing were observed, but with few differences between them and with minor differences in force distribution. Apparently, the teeth configuration in one or two stages was not effective, i.e. on the initial machining or during punch withdrawal. This indicates that the most significant differences in the results obtained by Marcondes *et al.* [**12**] were due to combination with other variables such as lubrication and balanced convex shear of the punch.

3.1 Punch design study

As the geometries of the combined punching–broaching tools did not show significant differences in quality at the punched hole wall, four new punch types were proposed, as depicted in Fig. 4. In this section, the influence of such geometries on the hole quality and the force profile during the process is analysed. It is worthy of note that type IV is a punch with reduced tip contact area, type V is a punch with a reduced flat face (two cutting steps), type VI has conic broaching teeth, and type VII has a concave conic shear angle of 22.5º [**10**]. The FEM model was built as described in section 2.

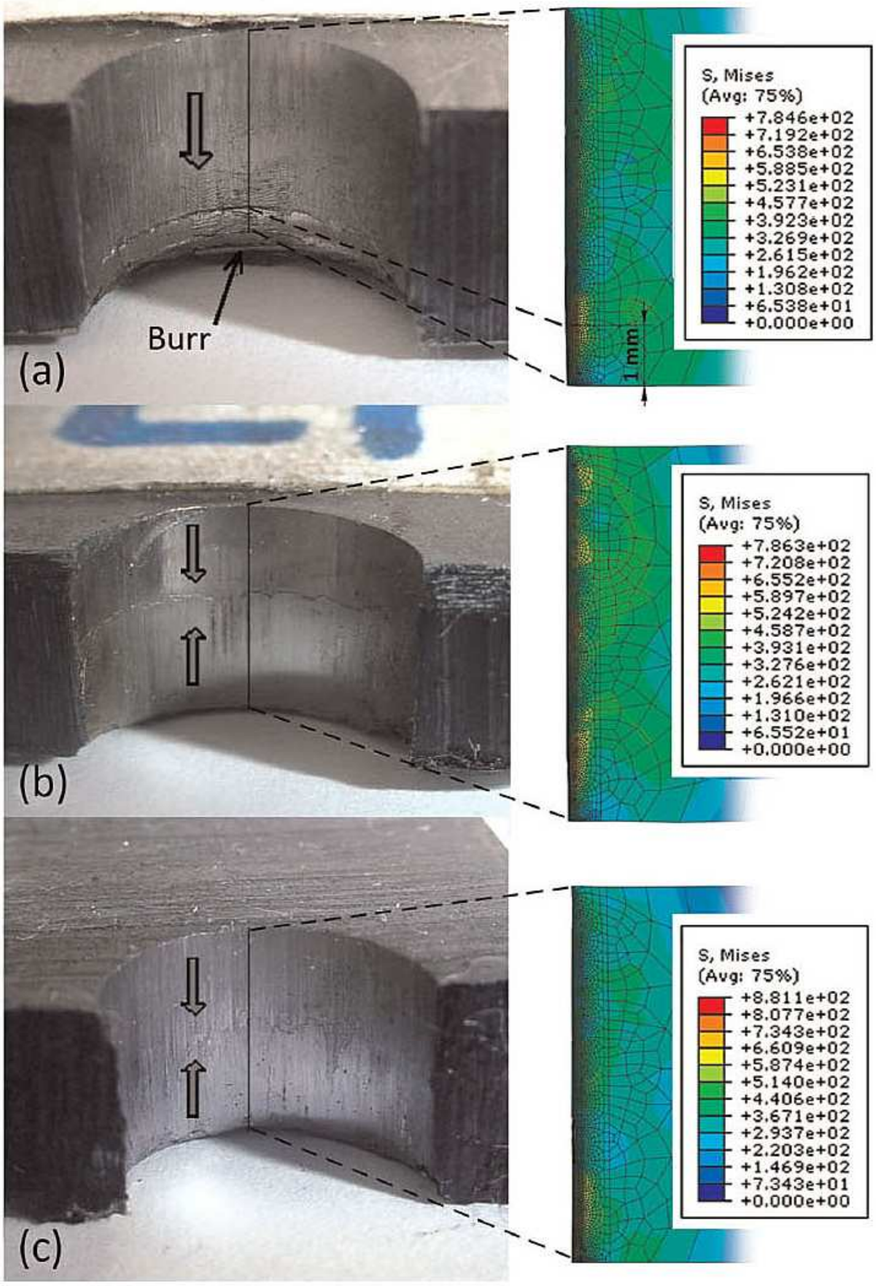

Fig. 2 Hole wall quality obtained with the different punches: (a) type I; (b) type II; (c) type III

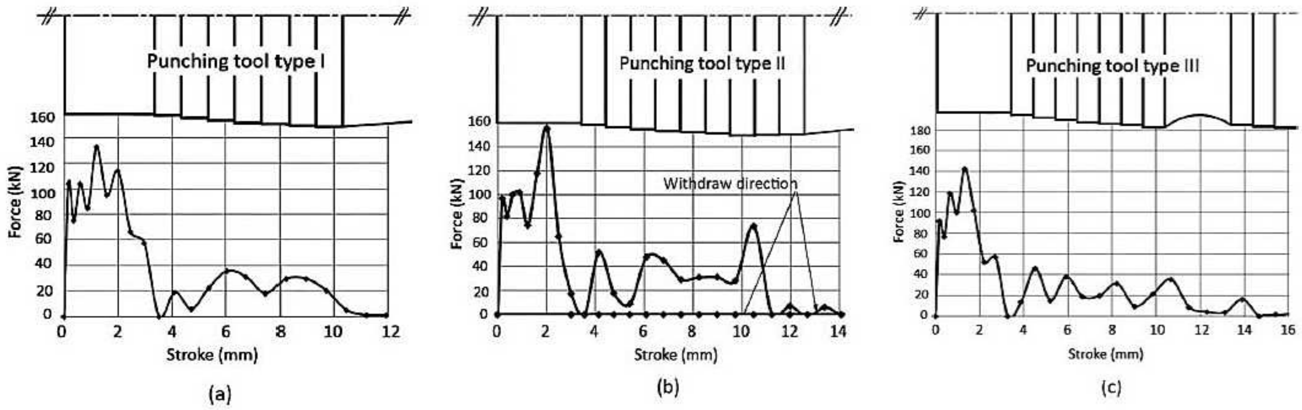

Fig. 3 Force versus stroke diagrams for the punching tools: (a) type I; (b) type II; (c) type III

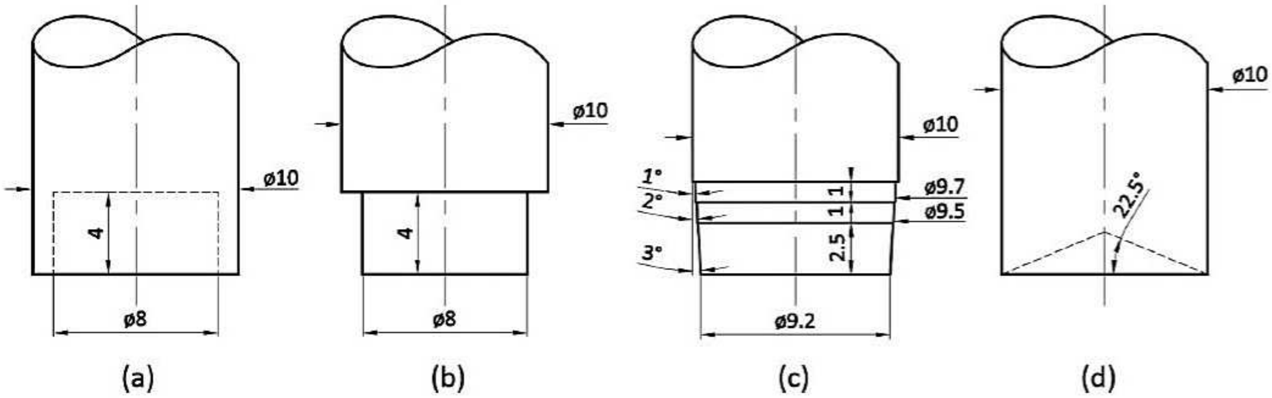

Fig. 4 New punch designs investigated (all dimensions in mm): (a) type IV; (b) type V; (c) type VI; (d) type VII

Figure 5 shows the influence of the different punch geometries on the punched hole wall and the force profile during the process. Punch types IV, V, and VI showed the maximum force located at 1 mm stroke, i.e. the instant prior to the propagation of the superior and inferior cracks.

The type VII punch produced a more homogeneous force profile and with less initial ramp, with the force peak at 2 mm stroke and without sudden changes on the force profile. Such a characteristic suggests a smooth shearing operation brought about by the sharp angle at the cutting edge. In addition, the conic geometry showed a more uniform energy distribution. For type IV, V, and VI punches, the blow-out effect was expected at around one-third thickness (2.6 mm). However, probably due to their reduced tip area, a sudden blow-out effect was produced after 2 mm stroke.

The force–penetration data for type IV and V punches showed smaller forces with maximum value peaks of 90 and 100 kN, respectively, which is probably due to the smaller area in contact with the sheet until the occurrence of the fracture.

Type IV, V, and VI punches presented a force–stroke profile quite different from that shown by punch VII, which is attributed to the greater complexity of their geometries. Punch VI, for example, gradually penetrated the sheet with three broaching teeth acting on the hole wall. The beginning of the inferior crack was preceded by a force peak of 180 kN (1.2 mm stroke). The conicity of the punch tip made the main cutting edge have a smaller diameter (Ø9.2 mm at the tip of the punch) and, consequently, a bigger clearance between the punch and die of 5 per cent (0.4 mm). This larger clearance delayed the beginning of the inferior crack and also produced a larger fracture angle. However, after the total fracture at one-third thickness, the remaining broaching teeth machined the hole wall, producing a larger cylindrical region. It can be pointed out that the good action of the broaching teeth was shown in the force profile of the type VI punch delaying the force application point.

3.2 Innovative punch design

Based on such results, a novel punch geometry that combines the major advantages of the punches studied previously was proposed (Fig. 6). The conicity on the tip of the punch was designed to ease the initial penetration, producing a more homogeneous force profile. The shearing angle is t degrees, where t is the sheet thickness. For this new tool, four broaching teeth were designed at the punch body to machine the hole wall and gradually decrease the conicity. Also, the area near the punch tip was designed as a straight region with the size of one-third of the sheet thickness. It can be pointed out that this height assures that the first broaching tooth machines only after the occurrence of the blow-out effect – usually after one-third of punch penetration. The die diameter (ØD) was defined by equation (6)

$$\varnothing \mathrm{D} = \varnothing \mathrm{bp} + C_{\mathrm{f}} \tag{6}$$

where Øbp is the largest punch diameter and C_{f} is the punch die clearance of 0.2 per cent per side (0.016 mm) – ØD of 10.032 mm. The Øbp was defined for punching holes of 10 mm diameter on 8 mm thick steel sheet. The diameter at the punch tip was defined according to equation (7)

$$\varnothing \mathrm{pt} = \varnothing \mathrm{D} - (C_0 \times 2) \tag{7}$$

where the initial clearance per side between the die and the region at the punch tip, C_0, was defined as 7 per cent, resulting in Øpt of 8.91 mm. At the region between Øbp and Øpt, four broaching teeth were

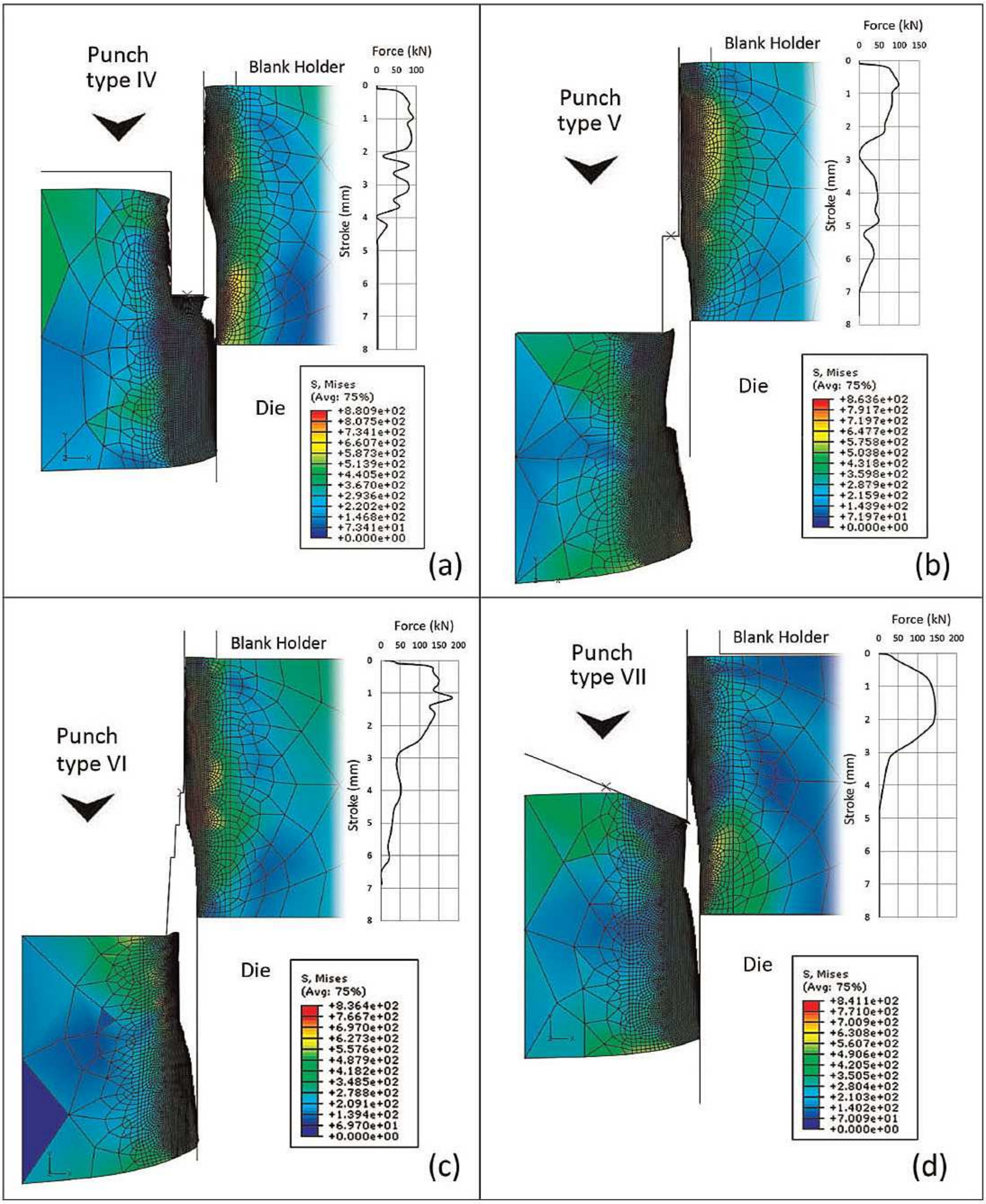

Fig. 5 Stroke versus force for different punch designs (FEM): (a) type IV; (b) type V; (c) type VI; (d) type VII

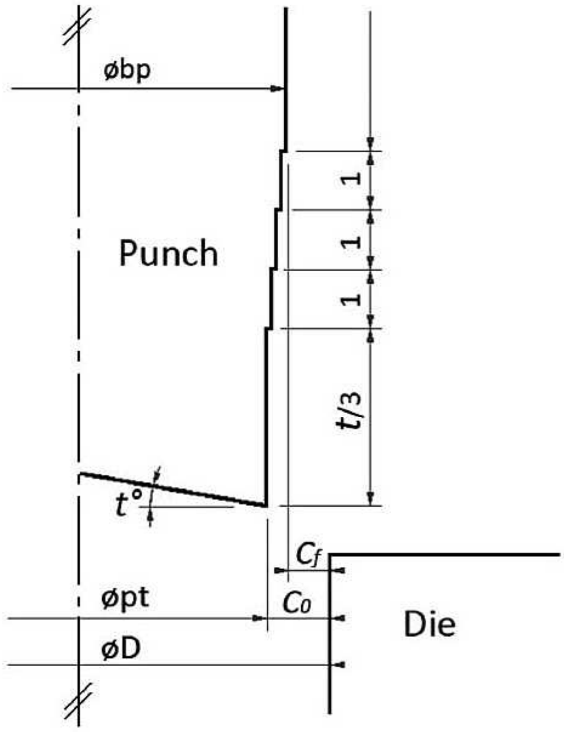

Fig. 6 Innovative punch design that assures the clearance variation between the punch and the die during punch penetration

defined with the objective of machining the remaining material to assure roundness of the hole.

3.3 Influence of punch geometry and the clearance variation during the process

Figure 7 shows the action of the proposed format at five different strokes. It can be observed that at 2.5 mm stroke – one-third of the sheet thickness – the superior and inferior cracks met each other and the blow-out effect took place. At this moment, the clearance between the punch and the die was 7 per cent causing a larger fracture angle.

Right after the blow-out, the first broaching tooth began to machine the hole wall. After 5.5 mm stroke, the last broaching tooth removed the remaining material. At this moment, the clearance between the punch and the die was 0.2 per cent, which produces a quite good cylindrical hole. The progressive clearance variation proposed for this punch, ranging from 7 per cent at its beginning to 0.2 per cent to its end, is crucial because the larger clearance proposed initially produces a larger fracture angle and leaves a large amount of material to be removed by the broaching teeth.

Besides reducing the punch force (100 kN maximum), the progressive action of the broaching teeth removes material with a lower force. The progressive reduction of the clearance during the process brought about a machining with the last tooth of the broach, with a clearance of just 0.2 per cent ensuring quite good cylindricity of the hole.

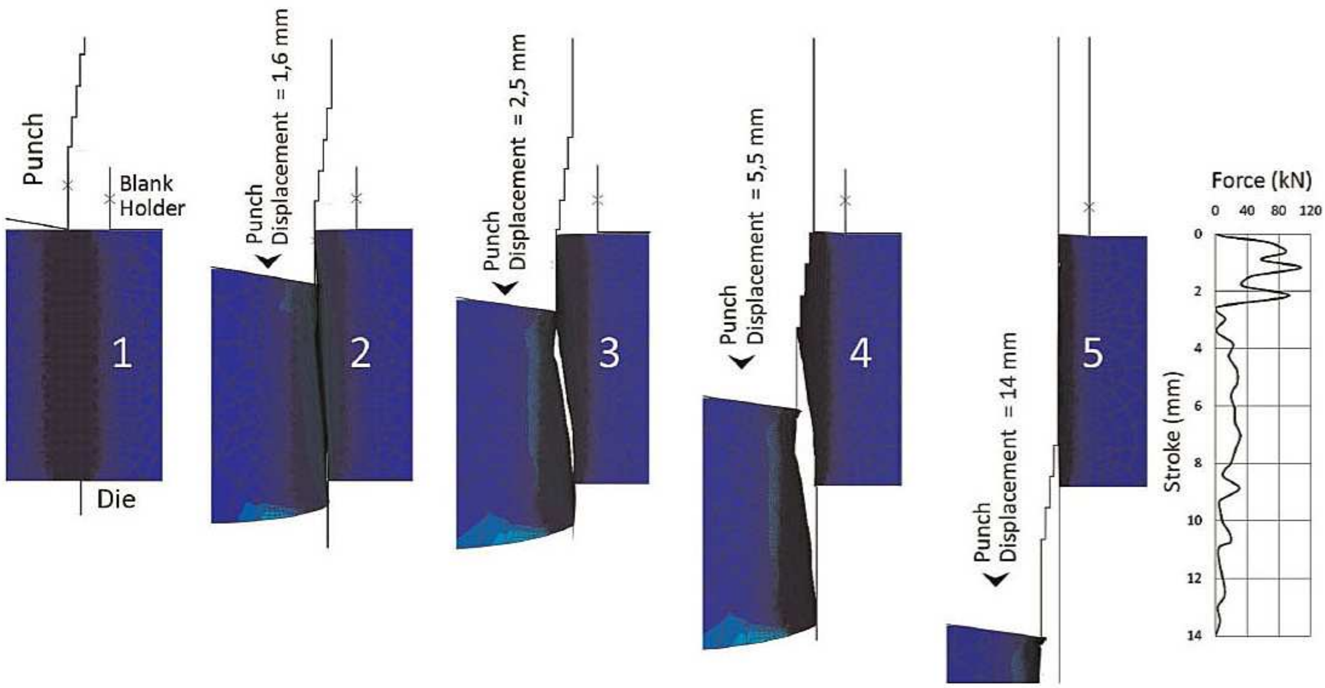

Fig. 7 Five steps of the innovative punching process

4 DISCUSSION

The numerical simulations with punches I, II, and III showed that the broaching teeth configuration did not cause any differences in hole wall quality, indicating that the most significant differences in the results obtained by Marcondes *et al.* [**12**] were due to combination with other variables such as lubrication and balanced convex shear of the punch. However, from the punch design study in section 3.1, it was possible to observe the real influence of punch geometry on the shearing edge quality, such as:

(a) the smoothing of the force curve and the more uniform energy distribution caused by punch type VII;
(b) the lowest levels of force that were achieved with punch types IV and V due to the smaller area in contact with the sheet until the occurrence of the fracture;
(c) the large burnish area produced by punch type VI that was achieved due a larger clearance on the tip of the punch, i.e. producing a larger fracture angle that keeps more material which is gradually removed by penetration of the three broaching teeth.

All of this information was helpful to design the innovative punch proposed in section 3.2. As can be seen, the present work has defined dimensions that are parameterized based on the thickness of the sheet to be punched. In addition, this innovative punch configuration showed a completely cylindrical hole.

5 CONCLUSIONS

The computational simulation of the punching process proved to be efficient to aid the optimization of the tool geometry and process parameters. The combined punching–broaching process was successfully simulated and revealed only small differences between the three initial proposed geometries (types I, II, and III). On the other hand, the simulations with punches IV, V, VI, and VII showed how the punch geometry can significantly affect the hole quality and the forces during the punching–broaching process. A novel punch with the beneficial characteristics of these studied punches was additionally proposed. The parametric configuration of this innovative punch facilitates the definition of the dimensions of the tool based on the thickness of the sheet and can allow the punching of holes with excellent roundness. However, it should be highlighted that the results of the present work are valid only for punching thick sheets of NBR 6656 steel.

FUNDING

This work was supported by CAPES (Brazil).

REFERENCES

1 **Al-Momani, E.** and **Rawabdeh, I.** An application of finite element method and design of experiments in the optimization of sheet metal blanking process. *J. Mech. Ind. Engng*, 2008, **2**, 53–63.
2 **Hatanaka, N., Yamaguchi, K.,** and **Takakura, N.** Finite element simulations of the shearing mechanism in the blanking of sheet metal. *J. Mater. Process. Technol.*, 2003, **139**, 64–70.
3 **Husson, C., Correia, J. P. M., Daridon, L.,** and **Ahzi, S.** Finite elements simulations of thin copper sheets blanking: study of blanking parameters on sheared edge quality. *J. Mater. Process. Technol.*, 2008, **199**, 74–83.
4 **Soares, J. A., Gipiela, M. L., Lajarin, S. F.,** and **Marcondes, P. V. P.** Study of the punch–die clearance influence on thick sheets sheared edge quality. *Int. J. Adv. Mfg Technol.*, 2011, in press.
5 **Hambli, R.** Design of experiment based analysis for sheet metal blanking processes optimization. *Int. J. Adv. Mfg Technol.*, 2002, **19**, 403–410.
6 **Hambli, R., Potiron, A.,** and **Kobi, A.** Application of design of experiment technique for metal blanking processes optimization. *Mec. Ind.*, 2003, **4**, 175–180.
7 **Marouani, H.,** et al. Numerical investigations on sheet metal blanking with high speed deformation. *Mater. Des.*, 2009, **30**, 3566–3571.
8 **Komori, K.** Simulation of shearing by node separation method. *Comput. Struct.*, 2001, **76**, 197–207.
9 **Farzin, M., Javani, H. R., Mashayekhi, M.,** and **Hambli, R.** *J. Mater. Process. Technol.*, 2006, **177**, 287–290.
10 **Singh, U. P., Streppel, A. H.,** and **Kals, H. J. J.** Design study of the geometry of a punching/blanking tool. *J. Mater. Process. Technol.*, 1992, **33**, 331–345.
11 **Mello, L. B.** and **Marcondes, P. V. P.** Punching and broaching combos – a new stamping tool. *J. Braz. Soc. Mech. Sci. Engng*, 2006, **28**, 94–98.
12 **Marcondes, P. V. P., Eto, A. M., Beltrão, P. A. C.,** and **Borges, P. C.** A smart stamping tool for punching and broaching combination. *J. Mater. Process. Technol.*, 2008, **206**, 188–193.
13 **Anon**. *ABAQUS/CAE user's manual, version 6.9*, 2009.
14 **Söderberg, M.** *Finite element simulation of punching*. Dissertation, Luleå University of Technology, Luleå, Sweden, 2006.
15 **Wu, T.-T.** A proposed methodology for strain-based failure criteria. In Proceedings of PVP2008-61572, 2008 ASME Pressure Vessels and Piping Division Conference, Chicago, Illinois, 27–31 July 2008.